Integral cross sections for the direct excitation of the A $^3\Sigma_u^+$, B $^3\Pi_g$, W $^3\Delta_u$, B′ $^3\Sigma_u^-$, a′ $^1\Sigma_u^-$, a $^1\Pi_g$, w $^1\Delta_u$, and C $^3\Pi_u$ electronic states in N_2 by electron impact

P. V. Johnson, C. P. Malone, and I. Kanik
Jet Propulsion Laboratory, California Institute of Technology, Pasadena, California, USA

K. Tran and M. A. Khakoo
Department of Physics, California State University, Fullerton, Fullerton, California, USA

Received 21 June 2005; revised 19 August 2005; accepted 7 September 2005; published 30 November 2005.

[1] Integral cross sections for electron impact excitation out of the ground state (X $^1\Sigma_g^+$) to the A $^3\Sigma_u^+$, B $^3\Pi_g$, W $^3\Delta_u$, B′ $^3\Sigma_u^-$, a′ $^1\Sigma_u^-$, a $^1\Pi_g$, w $^1\Delta_u$, and C $^3\Pi_u$ states in N_2 are reported at incident energies ranging between 10 and 100 eV. These data have been derived by integrating differential cross sections previously reported by this group. New differential cross section measurements for the a $^1\Pi_g$ state at 200 eV are also presented to extend the range of the reported integral cross sections for this state, which is responsible for the emissions of the Lyman-Birge-Hopfield band system (a $^1\Pi_g \rightarrow$ X $^1\Sigma_g^+$). The present results are compared and critically evaluated against existing cross sections. In general, the present cross sections are smaller than previous results at low impact energies from threshold through the excitation function peak regions. These lower cross sections have potentially significant implications on our understanding of UV emissions in the atmospheres of Earth and Titan.

Citation: Johnson, P. V., C. P. Malone, I. Kanik, K. Tran, and M. A. Khakoo (2005), Integral cross sections for the direct excitation of the A $^3\Sigma_u^+$, B $^3\Pi_g$, W $^3\Delta_u$, B′ $^3\Sigma_u^-$, a′ $^1\Sigma_u^-$, a $^1\Pi_g$, w $^1\Delta_u$, and C $^3\Pi_u$ electronic states in N_2 by electron impact, *J. Geophys. Res.*, *110*, A11311, doi:10.1029/2005JA011295.

1. Introduction

[2] Molecular nitrogen is the main atmospheric constituent of Earth, Titan, and Triton. Electron collisions with this molecule are responsible for much of the observed emission in the Earth's dayglow, nightglow, and aurora. Further, the successful insertion of the Cassini spacecraft into orbit around Saturn in July 2004, and the subsequent and continuing observations of Titan's atmosphere with the onboard Ultraviolet Imaging Spectrograph, make the determination of accurate N_2 excitation cross sections particularly timely. In order to properly account for the energy flow through the excited states of N_2 in these environments, accurate cross sections of as many processes involving N_2 as possible are required.

[3] Generally speaking, the cross sections needed for detailed analysis of atmospheric emissions are determined via electron impact induced optical emission spectroscopy (i.e., emission cross sections, ECSs) or by integrating electron scattering differential cross sections (DCSs) determined through electron energy loss spectroscopy to produce integral cross sections (ICSs). Of the two methods, ICSs are often preferred as they are restricted to direct excitation of the level in question, whereas ECSs, which concern the observation of emitted photons, involve direct excitation as well as cascade from higher-lying levels and branching decay channels (radiative, predissociation) that take part in the photoemission process. However, in the case of N_2, many of the states of interest are associated with overlapping spectral features in the energy loss spectrum. Therefore the accuracy of the derived ICSs is heavily dependent on the spectral energy resolution and quality and underlying assumptions pertaining to the spectral unfolding methods.

[4] To date, the pioneering work of *Cartwright et al.* [1977a, 1977b], whose data were later renormalized by *Trajmar et al.* [1983], and that of *Campbell et al.* [2001] are the only comprehensive experimental determinations of ICSs for the states examined in the present work (these works were extended further to include the E $^3\Sigma_g^+$ and a″ $^1\Sigma_g^+$ states). Apart from these measurements, various ICSs have been determined for subsets of these states by, for instance, *Brinkman and Trajmar* [1970] (a $^1\Pi_g$), *Finn and Doering* [1976] (a $^1\Pi_g$), *Zetner and Trajmar* [1987] (A $^3\Sigma_u^+$, B $^3\Pi_g$, W $^3\Delta_u$, a $^1\Pi_g$), and *Zubek and King* [1994] (C $^3\Pi_u$). Detailed reviews of existing N_2 cross sections are given by *Trajmar et al.* [1983], *Trajmar and Cartwright* [1984], *Itikawa et al.* [1986], *Zecca et al.* [1996], *Brunger and Buckman* [2002], *Brunger et al.* [2003], and *Itikawa* [2005].

[5] *Khakoo et al.* [2005] have recently measured DCSs over an extended range of incident energies for the eight

0148-0227/05/2005JA011295$09.00

lowest excited electronic states of N_2. These measurements are expected to be an improvement over previous measurements and *Khakoo et al.* [2005] provide arguments, which will be discussed in the following section, to support the improved accuracy of their results over other available DCSs from which other existing ICSs are derived. As such, it was important to derive new ICSs from these data.

[6] The DCSs of *Khakoo et al.* [2005] covered a range in energy loss spanning 6.25 to 11.25 eV. This range in energy loss allowed for the extraction of DCSs, and thereby the present ICSs, for the electron impact excitation of the A $^3\Sigma_u^+$, B $^3\Pi_g$, W $^3\Delta_u$, B′ $^3\Sigma_u^-$, a′ $^1\Sigma_u^-$, a $^1\Pi_g$, w $^1\Delta_u$, and C $^3\Pi_u$ electronic levels out of the X $^1\Sigma_g^+$ ground state. These excitation processes play important roles in a number of prominent N_2 emissions. Perhaps most notable is the excitation of the a $^1\Pi_g$ state whose transition to the ground state results in the ultraviolet (UV) emissions of the Lyman-Birge-Hopfield (LBH) system. The excitation of the a′ $^1\Sigma_u^-$ and w $^1\Delta_u$ states, which have been suggested to populate the a $^1\Pi_g$ level through radiative and collisionally induced cascade and thereby contribute to the LBH emission (a′-a-X, w-a-X, and a′-w′-a-X), are also of particular importance. Excitation of the A $^3\Sigma_u^+$, B $^3\Pi_g$, and C $^3\Pi_u$ states gives rise to the emissions of the Vegard-Kaplan system (A $^3\Sigma_u^+$ - X $^1\Sigma_g^+$), which are observed in the aurora, and the first (B $^3\Pi_g$ - A $^3\Sigma_u^+$) and second (C $^3\Pi_u$ - B $^3\Pi_g$) positive systems that together dominate N_2 emissions throughout the visible and near-infrared. Further, these three states, along with the W $^3\Delta_u$ and B′ $^3\Sigma_u^-$ states, account for a number of interconnecting cascade pathways to the ground state (e.g., C-B-A-X, C-A-X, B′-B-A-X, W-A-X, B-A-X) [*Lofthus and Krupenie*, 1977].

2. Differential Cross Sections

[7] *Khakoo et al.* [2005] detail the experimental and analytical procedures used to determine the DCSs from which the ICSs presented here were derived. However, the quality of these DCS data and the associated uncertainties are directly reflected in the presently derived ICSs. Therefore a brief summary of the DCS measurements is given here and the reader is urged to refer to *Khakoo et al.* [2005] for details.

[8] Cylindrical electrostatic optics and double hemispherical energy selectors were utilized both in the electron gun and the detector (see *Khakoo et al.* [1994] for further details). Energy loss spectra, including both the elastic peak and the inelastic region of interest, were collected at fixed impact energies and scattering angles by repetitive, multichannel-scaling techniques. The target N_2 beam was formed by effusing the gas through a collimating capillary array. The background signal was accurately determined using a proven [*Johnson et al.*, 2003; *Childers et al.*, 2004] moveable target source method first described by *Hughes et al.* [2003].

[9] Energy loss spectra were accumulated over the energy loss range of 6.25 eV to 11.25 eV covering a maximum angular range of 5° to 130° in 5°–10° intervals. To establish a uniform transmission response of the spectrometer for scattered electrons, the spectrometer was tuned so that the scattered electron signal followed the same relative intensity as the time-of-flight (TOF) value (for gross features) accurately determined by *LeClair and Trajmar* [1996]. The measured spectra were then unfolded to obtain individual intensities of the A $^3\Sigma_u^+$, B $^3\Pi_g$, W $^3\Delta_u$, B′ $^3\Sigma_u^-$, a′ $^1\Sigma_u^-$, a $^1\Pi_g$, w $^1\Delta_u$, and C $^3\Pi_u$ states relative to the total summed intensity (A + W + B + B′ + a′ + a + w + C). The unfolding procedure made use of Franck Condon (FC) factors for X $^1\Sigma_g^+$ ($v'' = 0$) → n′ (v′) vibrational transitions to the n′ electronic manifold from a combination of sources [*Tanaka et al.*, 1964; *Benesch et al.*, 1965; *Cartwright et al.*, 1977a] according to procedures described by both *Wrkich et al.* [2002] and *Khakoo et al.* [2005].

[10] Additional energy loss spectra covering the elastic (−0.25 eV to +0.25 eV energy loss) and inelastic (6 eV to 11.5 eV energy loss) regions were measured using the moveable target source method. Total summed DCSs (A + W + B + B′ + a′ + a + w + C) were then obtained by (relatively) normalizing the elastic peak counts to an average of selected experimental DCSs for elastic electron scattering from N_2 [*Shyn and Carignan*, 1980; *Trajmar et al.*, 1983; *Nickel et al.*, 1988; *Gote and Ehrhardt*, 1995]. These (relative) summed DCS data were then placed on an absolute scale using the inelastic DCSs obtained from the TOF measurements of *LeClair and Trajmar* [1996] to correct for any variation in the analyzer response function between the elastic feature and the inelastic features under scrutiny. In this way, full DCSs for each electronic state over all v′ levels excitable at that electron energy were determined. For electron impact energies greater than 12.5 eV, the transmission correction (determined by comparing the experimental elastic to inelastic ratios with those given by *LeClair and Trajmar* [1996]) was <12%. At 10 and 12.5 eV impact energies, the variation in analyzer response was more significant (∼27% at 10 eV).

[11] The DCSs of each state were obtained by applying the earlier individual state fractional intensities obtained from the unfolding procedure to the normalized summed DCSs. Experimental errors were determined by combining all of the contributing error components in quadrature: (1) statistical and fitting errors in the individual scattering intensities (typically 2–30%), (2) inelastic/elastic ratio error of the TOF results (∼10%) [*LeClair and Trajmar*, 1996], (3) the error in the available elastic scattering DCSs (<15%), (4) the error propagated by the inelastic to elastic ratio measurements (typically 5%), (5) error introduced by the analyzer response function (10%), and (6) an uncertainty for the dependence of the flux-weighted FC factors on the electron residual energy (10% at E_0 = 10 eV, ∼8% at E_0 = 12.5 eV, greater than 5% at E_0 = 15 eV, and for E_0 > 15 eV this correction was negligibly small).

[12] There are several factors that should be kept in mind while assessing these DCSs in comparison with previous measurements. Although the elastic scattering DCSs that are available for N_2 are in good agreement (typically within 12%), the usual method of normalizing to elastic DCSs is hindered by background effects produced by elastically scattered secondary electrons from surfaces in the apparatus. Further, these effects compound at small angles where the detector provides an additional target for the incident electron beam. The recently developed moveable target source method employed by *Khakoo et al.* [2005] is able to accurately enable the determination of such backgrounds and hence can be expected to provide significantly improved results compared with previous investigations.

Table 1. DCSs for Electron Impact Excitation of the a $^1\Pi_g$ State From the X $^1\Sigma_g^+$ Ground State at 200 eV Impact Energy

Scattering Angle, degrees	DCS, $\times 10^{-18}$ cm^2 sr^{-1}	Error, $\times 10^{-18}$ cm^2 sr^{-1}
5	17.3	4.3
10	8.94	2.23
20	2.08	0.52
30	0.317	0.079
40	0.0873	0.0218
50	0.0348	0.0087
60	0.0236	0.0059
70	0.0216	0.0054
80	0.0139	0.0035
90	0.0108	0.0027
100	0.0109	0.0027
110	0.0126	0.0032
120	0.0183	0.0046

Furthermore, variation in the spectrometer response as a function of energy loss is also a concern when normalizing to an elastic feature that is up to ~11 eV away. However, this effect was minimized through tuning and later corrected for using the TOF experimental data of *LeClair and Trajmar* [1996] (as previously discussed).

[13] Apart from the results of *Khakoo et al.* [2005], new DCSs for the excitation a $^1\Pi_g$ were determined at 200 eV using the same apparatus and experimental techniques. However, a somewhat simpler method was used to extract the absolute DCSs from the energy loss spectra. At 200 eV, the DCSs for N_2 are relatively small, which makes collecting sufficient statistics for accurate spectral unfolding problematic. However, in considering the *Khakoo et al.* [2005] data, it was noted that the differential (angular) ratio of the a $^1\Pi_g$ DCS to total summed DCS was essentially the same, within ~10%, at 50 and 100 eV impact energies. This afforded a means of obtaining the 200 eV a $^1\Pi_g$ DCS while avoiding the aforementioned difficulties associated with small DCSs.

[14] Energy loss spectra were collected to determine the differential total summed intensities of the A $^3\Sigma_u^+$, B $^3\Pi_g$, W $^3\Delta_u$, B′ $^3\Sigma_u^-$, a′ $^1\Sigma_u^-$, a $^1\Pi_g$, w $^1\Delta_u$, and C $^3\Pi_u$ states at 5° and from 10° to 120° in 10° intervals. Then, by assuming that the trend in the ratio of the a $^1\Pi_g$ DCS to total summed DCS observed at 50 and 100 eV extended to 200 eV, the a $^1\Pi_g$ DCSs were extracted. In order to account for additional errors involved with the underlying assumption of this method, a further 10% uncertainty was assigned to the determined DCSs. These results are listed in Table 1 and are shown graphically in Figure 1.

3. Integral Cross Sections

[15] ICSs were derived from the DCSs of *Khakoo et al.* [2005] and the presently determined DCSs at 200 eV for excitation of the a $^1\Pi_g$ state by interpolating between measured DCSs and extrapolating to unmeasured scattering angles prior to integration. Interpolation between measured points was performed using a B-spline algorithm. It should be noted that apart from the B-spline interpolation, no smoothing of the DCS data was performed in either the *Khakoo et al.* [2005] or present analyses.

[16] Unfortunately, there is a distinct lack of ab initio theoretical DCS data available for the excitation processes studied here. Therefore without reliable theory to use as a guide, extrapolations of the DCSs to experimentally inaccessible scattering angles were performed based on trends observed in the DCS data. Although this procedure may seem ad hoc at first, the following arguments can be made to support the accuracy of the performed extrapolations. First, there was very little angular range over which the DCSs had to be extrapolated ($\Delta\theta = 5°–25°$ toward $\theta = 0°$ and $\Delta\theta = 50°$ toward 180°; $\Delta\theta = 60°$ in the case of the 200 eV a $^1\Pi_g$ DCSs). The low angle extrapolation may initially seem cause for concern given the forward peaked nature of some of the DCSs involved. However, when integrating the DCSs over all scattering angles to obtain ICSs, the $\sin\theta$ factor introduced in the differential volume element suppresses the contribution of the $\theta = 0°$ to 5° region of the DCS to the final ICS. Although this is also true as $\theta \rightarrow 180°$, the high angle extrapolations covered a much larger angular range (50°; 60° in the case of the 200 eV a $^1\Pi_g$ DCS). However, the forward peaked nature of some of the DCSs involved serves to minimize the contribution of the extrapolated regions.

[17] In order to estimate the uncertainty in the final ICSs, two further integrations were performed for each transition and energy in which extrapolations were made over the unmeasured angles by holding the DCSs at the lowest and highest measured angles constant (flat) down to 0° and up to 180°, respectively. The differences between the results of these integrations and the properly determined ICSs were taken to represent the uncertainties associated with each extrapolation. The two extrapolation uncertainties were then combined in quadrature to arrive at the net uncertainty contributed by the extrapolation procedure. Since DCSs were measured in small angular intervals (5°–10°), no uncertainty was attributed to the interpolation between

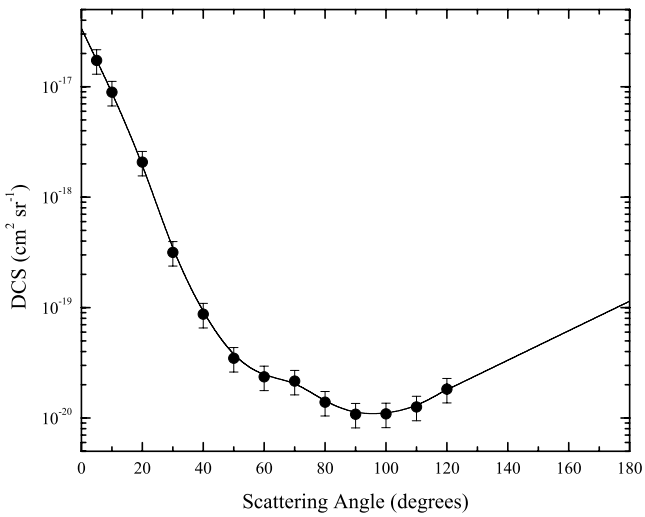

Figure 1. Differential cross sections (DCSs) for electron impact excitation (at $E_0 = 200$ eV) of the a $^1\Pi_g$ state from the X $^1\Sigma_g^+$ ground state (solid circles represent present data; solid line represents interpolation and extrapolation over unmeasured angles used to determine the integral cross sections (ICS)).

Table 2. ICSs for Electron Impact Excitation of the A $^3\Sigma_u^+$, B $^3\Pi_g$, W $^3\Delta_u$, B′ $^3\Sigma_u^-$, a′ $^1\Sigma_u^-$, a $^1\Pi_g$, w $^1\Delta_u$ and C $^3\Pi_u$ States From the X $^1\Sigma_g^+$ Ground State in N_2 ($\times 10^{-18}$ cm^2)[a]

Energy, eV	A $^3\Sigma_u^+$	B $^3\Pi_g$	W $^3\Delta_u$	B′ $^3\Sigma_u^-$	a′ $^1\Sigma_u^-$	a $^1\Pi_g$	w $^1\Delta_u$	C $^3\Pi_u$	Sum
10	23.2 ± 4.2	29.9 ± 5.5	1.85 ± 0.44	—	—	—	—	—	53.3 ± 9.5
12.5	12.4 ± 2.2	21.3 ± 3.6	11.3 ± 2.0	1.64 ± 0.43	1.49 ± 0.35	7.26 ± 1.25	0.689 ± 0.246	0.761 ± 0.171	56.8 ± 9.4
15	13.6 ± 2.5	15.0 ± 2.7	18.3 ± 3.4	5.07 ± 1.93	3.45 ± 0.97	16.1 ± 2.9	4.28 ± 0.83	17.1 ± 3.1	93.0 ± 16.3
17.5	11.9 ± 2.3	12.0 ± 2.1	17.8 ± 3.3	5.53 ± 2.12	3.18 ± 0.76	18.5 ± 3.3	3.94 ± 0.73	14.0 ± 2.5	86.8 ± 15.2
20	10.8 ± 2.1	12.2 ± 2.2	20.7 ± 3.8	5.82 ± 1.51	2.31 ± 0.63	21.0 ± 3.7	3.68 ± 0.71	10.6 ± 1.9	87.2 ± 15.3
30	6.88 ± 1.75	12.0 ± 2.1	7.54 ± 1.37	3.02 ± 0.78	2.07 ± 0.48	20.7 ± 3.4	1.87 ± 0.34	6.87 ± 1.13	61.0 ± 10.2
50	4.46 ± 1.39	4.43 ± 0.79	3.35 ± 0.58	1.30 ± 0.33	0.801 ± 0.196	13.0 ± 2.1	1.08 ± 0.23	3.00 ± 0.49	31.4 ± 5.2
100	0.910 ± 0.163	0.607 ± 0.110	0.703 ± 0.137	0.277 ± 0.096	0.251 ± 0.080	7.16 ± 1.29	0.749 ± 0.196	0.542 ± 0.097	11.2 ± 1.9
200	—	—	—	—	—	3.41 ± 0.87	—	—	—

[a]See the text in section 4.9 for further details regarding the "sum" cross section.

measured data points. Therefore the extrapolation uncertainties were combined in quadrature with the average uncertainties in the parent DCS data sets to provide error estimates in the ICS values. An example of a DCS interpolation/extrapolation is shown in Figure 1.

4. Results and Discussion

[18] The derived ICS values are listed in Table 2. The ICSs are also plotted in Figures 2–10 along with a selection of available experimental and theoretical results. In terms of ICSs derived from DCS measurements, the plots include ICSs recommended by *Trajmar et al.* [1983] (i.e., renormalized data of *Cartwright et al.* [1977b]; referred to as *Cartwright et al.* [1977b; *Trajmar et al.*, 1983] from here on) as well as all ICSs, at comparable energies, published since. Of note, in the original *Cartwright et al.* [1977b] paper, ICSs were only experimentally determined at impact energies of 10, 12.5, 15, 17, 20, 30, and 50 eV. However, depending on the threshold, ICSs were not determined at each of these energies for all included states. In addition, cross sections were reported at finer energy intervals and at lower energies than those for which experiments were performed through interpolations and extrapolations. Therefore care must be taken when considering these data, especially at low energies (i.e., <15 eV).

[19] For comparison with theory, the ICSs of *Gillan et al.* [1996] have been included. Earlier theoretical ICSs have been discussed by *Gillan et al.* [1996] and these other theoretical ICSs have not been included here with the exception of *Chung and Lin*'s [1972] calculated ICSs based on the Born approximation. Since these Born-derived ICSs are expected to provide reasonable results at high impact energies, they have been included where available. Further, since *Gillan et al.* [1996] did not provide ICSs for the X $^1\Sigma_g^+$ – a $^1\Pi_g$ transition, the calculation of *Holley et al.* [1981] has been included in this case. For more complete reviews of previous experimental and theoretical results please see the articles and reviews referenced in section 1.

[20] Unless otherwise noted, the discussed experimental ICS data were derived from DCS measurements in a manner similar to the present data. However, previous DCS measurements are generally plagued by old and inaccurate normalization standards and methods, ineffective angular coverage, insufficient energy resolution, and inadequate spectral unfolding. The present work was in part motivated by the varying collections of N_2 DCS and ICS data (for example, *Zetner and Trajmar* [1987] in the work of *Brunger and Buckman* [2002] and Trajmar private communications such as in the work of *Huo and Dateo* [1999]) assembled by the JPL group over numerous years, following the revised values by *Trajmar et al.* [1983]. The present work, along with the DCSs of *Khakoo et al.* [2005], is meant to supersede these previous data. In the cases where published data were determined by other experimental means, such as fluorescence emission techniques, this is explicitly stated in the text.

[21] Apart from the above techniques, ICSs can be derived from electron swarm measurements. However, application of this technique to molecular species becomes limited as the number of accessible inelastic channels increases. Under these circumstances, the strength of the swarm technique is in its ability to test the consistency of a proposed set of cross sections (e.g., elastic, inelastic, and ionization cross sections) and not to accurately determine the individual cross section for a specific process [*Brunger*

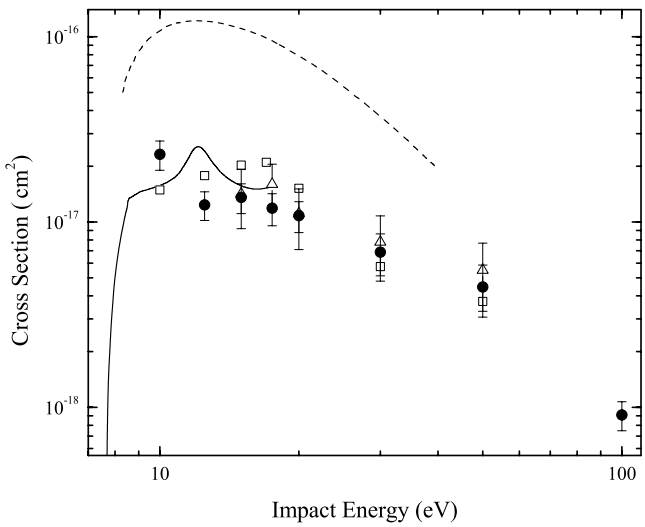

Figure 2. ICSs for electron impact excitation of the X $^1\Sigma_g^+$ - A $^3\Sigma_u^+$ transition in N_2 (solid circles represent present data, open squares represent *Cartwright et al.* [1977b] renormalized by *Trajmar et al.* [1983], open triangles represent *Campbell et al.* [2001], dash line represent *Chung and Lin* [1972], and solid line represents *Gillan et al.* [1996]).

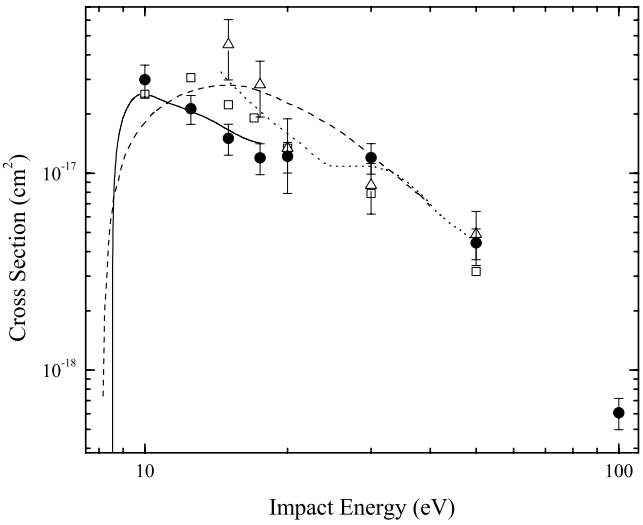

Figure 3. ICSs for electron impact excitation of the X $^1\Sigma_g^+$ - B $^3\Pi_g$ transition in N_2 (solid circles represent present data, open squares represent *Cartwright et al.* [1977b] renormalized by *Trajmar et al.* [1983], open triangles represent *Campbell et al.* [2001], dash line represents *Chung and Lin* [1972], solid line represents *Gillan et al.* [1996], and dot line represents *Fliflet et al.* [1979] scaled by 0.65).

et al., 2003]. Therefore such measurements are not well suited for direct comparison with the present data. Consequently, swarm results have been omitted from this discussion.

[22] It should be noted that in the cases where tabulations of published data were not available [*Holland*, 1969; *Chung and Lin*, 1972; *Fliflet et al.*, 1979; *Holley et al.*, 1981; *Gillan et al.*, 1996], data were digitized from published plots and included in the present figures for comparison. In the figures the digitized data points have been connected using either straight lines or B-spline interpolations to present smooth curves.

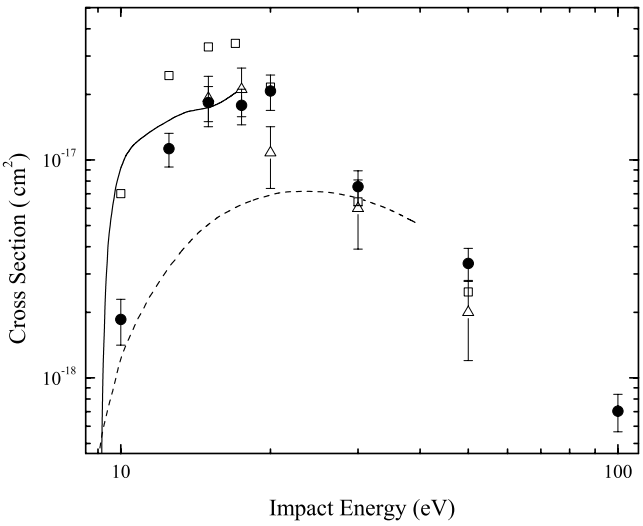

Figure 4. ICSs for electron impact excitation of the X $^1\Sigma_g^+$ - W $^3\Delta_u$ transition in N_2 (solid circles represent present data, open squares represent *Cartwright et al.* [1977b] renormalized by *Trajmar et al.* [1983], open triangles represent *Campbell et al.* [2001], dash line represents *Chung and Lin* [1972], and solid line represents *Gillan et al.* [1996]).

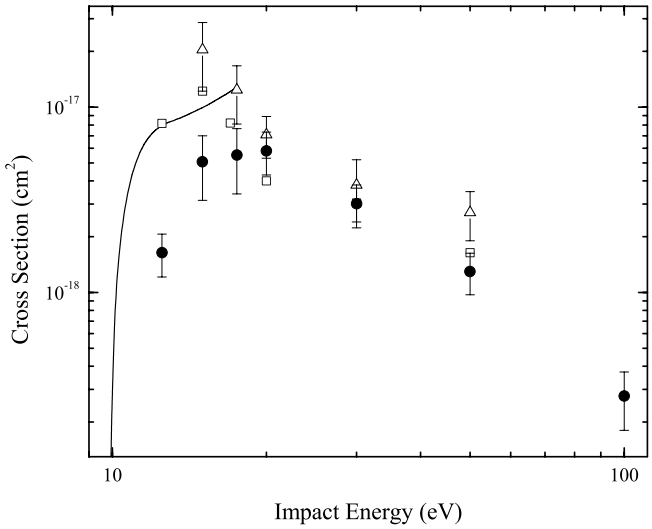

Figure 5. ICSs for electron impact excitation of the X $^1\Sigma_g^+$ - B′ $^3\Sigma_u^-$ transition in N_2 (solid circles represent present data, open squares represent *Cartwright et al.* [1977b] renormalized by *Trajmar et al.* [1983], open triangles represent *Campbell et al.* [2001], and solid line represents *Gillan et al.* [1996]).

4.1. X $^1\Sigma_g^+$ - A $^3\Sigma_u^+$

[23] ICSs for the excitation of the A $^3\Sigma_u^+$ state are shown in Figure 2. Relatively good agreement is seen among the experimental data sets over the whole energy range. The R-matrix calculation [*Gillan et al.*, 1996] predicts ICSs that

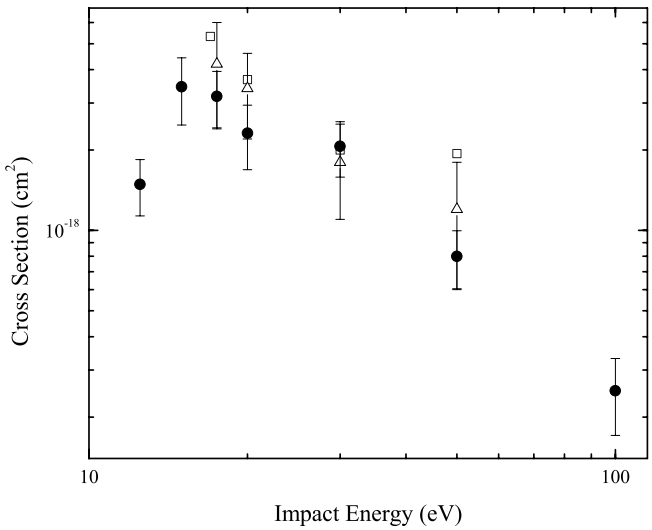

Figure 6. ICSs for electron impact excitation of the X $^1\Sigma_g^+$ - a′ $^1\Sigma_u^-$ transition in N_2 (solid circles represent present data, open squares represent *Cartwright et al.* [1977b] renormalized by *Trajmar et al.* [1983], and open triangles represent *Campbell et al.* [2001]).

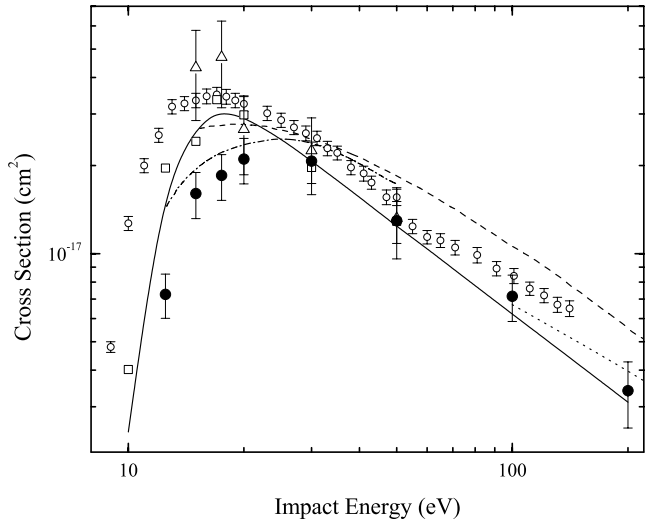

Figure 7. Cross sections for electron impact excitation of the X $^1\Sigma_g^+$ - a $^1\Pi_g$ transition in N_2 (solid circles represent present data, open squares represent *Cartwright et al.* [1977b] renormalized by *Trajmar et al.* [1983], open triangles represent *Campbell et al.* [2001], dash line represents *Chung and Lin* [1972], dash dot line represents *Holley et al.* [1981], dot line represents *Holland* [1969], solid line represents *Ajello and Shemansky* [1985], and open circles represent *Mason and Newell* [1987]).

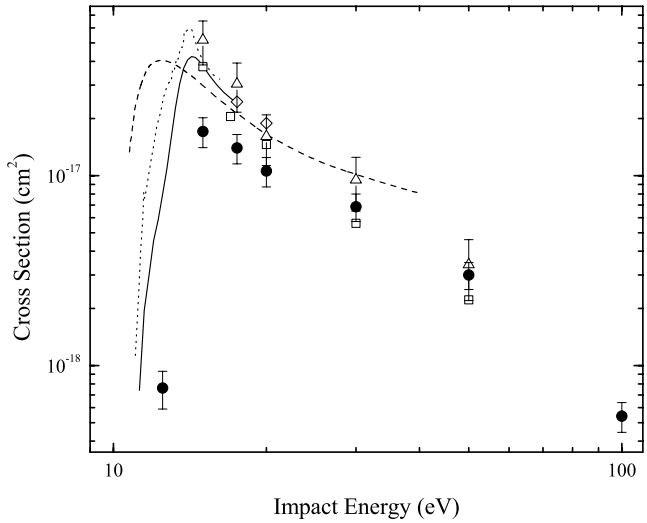

Figure 9. Cross sections for electron impact excitation of the X $^1\Sigma_g^+$ - C $^3\Pi_u$ transition in N_2 (solid circles represent present data, open squares represent *Cartwright et al.* [1977b] renormalized by *Trajmar et al.* [1983], open diamond represents *Zubek and King* [1994], open triangles represent *Campbell et al.* [2001], dash line represents *Chung and Lin* [1972], dot line represents *Poparic et al.* [1999], and solid line represents *Zubek* [1994]).

have good agreement with the available experiments. However, the small resonance structure (belonging to the formation of the N_2^- $1\pi_u^3$ $1\pi_g^2$ $^2\Pi_u$ complex) predicted near 12 eV is not observed in the experimental data sets. Interestingly, our raised ICS at 10 eV alludes somewhat to the existence of this resonance, but unfortunately this single point is insufficient to definitively identify the resonance. The Born-Ochkur results [*Chung and Lin*, 1972] are almost an order of magnitude larger than experimental results.

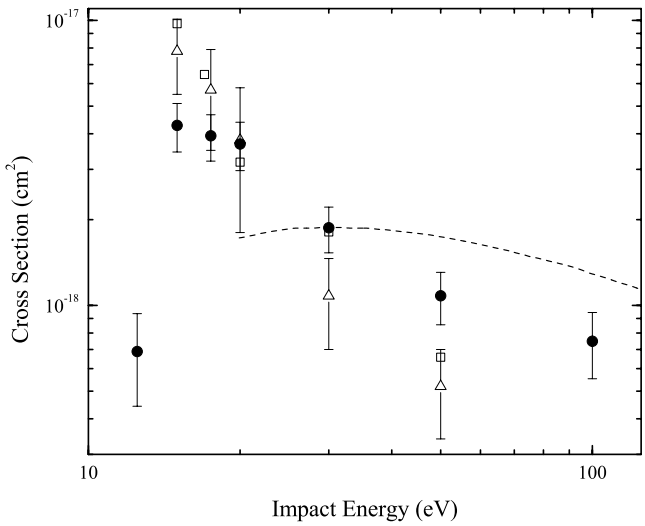

Figure 8. ICSs for electron impact excitation of the X $^1\Sigma_g^+$ - w $^1\Delta_u$ transition in N_2 (solid circles represent present data, open squares represent *Cartwright et al.* [1977b] renormalized by *Trajmar et al.* [1983], open triangles represent *Campbell et al.* [2001], and dash line represents *Chung and Lin* [1972]).

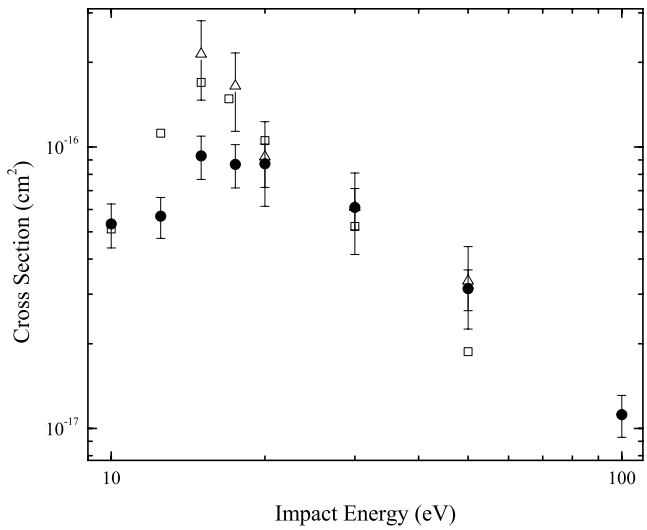

Figure 10. The summed ICSs for electron impact excitation of the X $^1\Sigma_g^+$ to A $^3\Sigma_u^+$, B $^3\Pi_g$, W $^3\Delta_u$, B′ $^3\Sigma_u^-$, a′ $^1\Sigma_u^-$, a $^1\Pi_g$, w $^1\Delta_u$ and C $^3\Pi_u$ states (solid circles represent present data, open squares represent *Cartwright et al.* [1977b] renormalized by *Trajmar et al.* [1983], and open triangles represent *Campbell et al.* [2001]). See the text for further details.

However, the shape of the excitation function shows a tendency to asymptote toward agreement at higher energies.

4.2. $X\ ^1\Sigma_g^+ - B\ ^3\Pi_g$

[24] Figure 3 shows the experimental and theoretical ICSs for excitation of the $B\ ^3\Pi_g$ state. Very good agreement is seen among the experimental data sets at energies $\geq$20 eV. Good agreement is seen with the renormalized data of *Cartwright et al.* [1977b; *Trajmar et al.*, 1983], whereas the *Campbell et al.* [2001] results grow to a factor of approximately three greater than the present data at the peak value ($\sim$15 eV). The *Gillan et al.* [1996] calculation gives excellent agreement with the present data, while *Chung and Lin* [1972] predict a broader peak in the excitation function that is shifted toward higher energy and suggests agreement at larger energies. Of interest and significance is the distorted-wave calculation (an intermediate energy model) of *Fliflet et al.* [1979] that reproduces the ''shoulder'' observed in the present ICSs near 30 eV. Therefore their $B\ ^3\Pi_g$ state cross section has been included in Figure 3 after being scaled by a factor of 0.65 to bring it in line with the present data at 50 eV. The overestimation toward threshold was expected and discussed by *Fliflet et al.* [1979].

4.3. $X\ ^1\Sigma_g^+ - W\ ^3\Delta_u$

[25] As seen in Figure 4, the present $X\ ^1\Sigma_g^+ - W\ ^3\Delta_u$ cross section data are in excellent accord with those of *Campbell et al.* [2001] over the entire energy range with the exception at 20 eV where the experimental error bars do not overlap. At 20 eV and above, the *Cartwright et al.* [1977b; *Trajmar et al.*, 1983] data agree well within error estimates with the present data but are significantly larger at lower energies. Again, the *Gillan et al.* [1996] results follow the trend in the present data while the *Chung and Lin* [1972] results substantially underestimate the cross sections in the threshold region but suggest convergence at larger energies.

4.4. $X\ ^1\Sigma_g^+ - B'\ ^3\Sigma_u^-$

[26] Figure 5 shows that experimental ICSs for excitation of the $B'\ ^3\Sigma_u^-$ state are in reasonably consistent agreement at 20 eV and above. However, the present data show a slower rise from threshold with a peak cross section some 5 eV above the peaks seen in the other experimental data sets. R-matrix calculations of *Gillan et al.* [1996] are in disagreement with the present data for this transition. The calculated ICSs are approximately a factor of 2 larger than the present data and show a somewhat sharper rise from threshold.

4.5. $X\ ^1\Sigma_g^+ - a'\ ^1\Sigma_u^-$

[27] The experimental ICSs measured by *Cartwright et al.* [1977b; *Trajmar et al.*, 1983] and *Campbell et al.* [2001] for the $X\ ^1\Sigma_g^+ - a'\ ^1\Sigma_u^-$ transition show good agreement, generally within the range of estimated uncertainties of the present data (Figure 6). However, they both indicate larger cross section peak values than the present data.

4.6. $X\ ^1\Sigma_g^+ - a\ ^1\Pi_g$

[28] Figure 7 shows that the experimental $X\ ^1\Sigma_g^+ - a\ ^1\Pi_g$ ICSs of *Cartwright et al.* [1977b; *Trajmar et al.*, 1983] and *Campbell et al.* [2001] agree well with the present data at 30 and 50 eV while the present data are significantly smaller closer to threshold. Note that a (presumed) transcription error was corrected in the *Trajmar et al.* [1983] tabulation (i.e., ICS = 12.9×10^{-18} cm^2 at 50 eV and not 2.9×10^{-18} cm^2).

[29] The Born approximation prediction [*Chung and Lin*, 1972] lies between the plotted data sets in the threshold to peak region and does not clearly converge toward the experimental data at high energy. However, the early, simple two-state close-coupling theoretical prediction of *Holley et al.* [1981] gives an excitation function that is similar in shape to the present data while lying at the upper reach of the estimated experimental uncertainties. Unfortunately, *Holley et al.* [1981] did not provide DCS results, which hinders a meaningful assessment of the calculation's accuracy.

[30] It is worthwhile to reconsider the Born-Ochkur (BO) data of *Chung and Lin* [1972] relative to the substantial number of data sets now available. The BO data plotted here and in other reviews were calculated by *Chung and Lin* [1972] using their wave function set (i). ICS data based on set (i) have presumably been favored over the others due to the reasonable agreement with the available and comparable experimental data of *Holland* [1969] and *Ajello* [1970]. ICS derived using wavefunction set (i) and set (iv) approximately lie on either side of the emission curve of *Holland* [1969] at large impact energies, while those derived using set (iv) have excellent agreement with the 100 eV data point of *Holland* [1969]. Examination of the emission data of *Ajello* [1970] shows a shape that is unacceptable at high energies, which was later attributed to the presence of secondary electrons in that experiment [*Finn and Doering*, 1976; *Ajello and Shemansky*, 1985]. On the basis of this exclusion, the present results set a preference of BO set (iv) ICSs over set (i) ICSs at ''high'' energies. However, BO set (iv) underestimates the cross section at low energy. Reconsideration of the choice of wavefunctions is prudent in light of the present direct measurement extending the ICSs to higher incident energies.

[31] Cross sections determined through fluorescence detection experiments by *Holland* [1969] and *Ajello and Shemansky* [1985] are included in Figure 7. *Holland* [1969] determined the ECSs at 100, 900, and 2000 eV by measuring emission intensities along a number of lines of sight perpendicular to the exciting electron beam to determine the total LBH emission. However, owing to the long lifetime of the $a\ ^1\Pi_g$ state, and the finite volume of the apparatus, a significant portion of the emission was not observed. By modeling the glow profile around the electron beam, the unobserved emission was accounted for and ECSs were determined. Holland did not account for predissociation in his ECS determination. However, if predissociation is factored into the *Holland* [1969] data set using the predissociation ($\sim$12%) suggested by *Ajello and Shemansky* [1985] for lower incident energies, then the Holland data agrees within errors with the present ICSs indicating that there is minimal cascade to the $a\ ^1\Pi_g$ state at high energy.

[32] *Ajello and Shemansky* [1985] measured LBH emission spectra as a function of impact energy from 120 to 210 nm, normalized using the cross section of Lyman α emission of H_2 [*Shemansky et al.*, 1985], and deduced ICSs for direct excitation of the $a\ ^1\Pi_g$ state using an analytical fit to the measured data. These results agree excellently with the present data at 30 eV and above.

Below this energy, the *Ajello and Shemansky* [1985] data lie above the present data but agree within stated errors at 20 eV and closely follow the results of *Cartwright et al.* [1977b; *Trajmar et al.*, 1983]. *Ajello and Shemansky* [1985] performed an analytical fit to their measured a $^1\Pi_g$ (3,0) (emission) excitation function, which indicated negligible cascade contribution. They further noted the strong, relative agreement between their emission excitation function and that of the original *Cartwright et al.* [1977b] data and a 5% absolute agreement in the ICSs from these two analyses. However, it should be pointed out that they did not take into account the renormalization by *Trajmar et al.* [1983] of the *Cartwright et al.* [1977b] data. The present results suggest a larger "fast" cascade contribution between threshold and peak to the a $^1\Pi_g$ emission than was concluded by *Ajello and Shemansky* [1985]. However, it should be noted that *Ajello and Shemansky* [1985] observed approximately a 10% and 17% deviation at incident energies 10 eV and 12 eV, respectively, between their (3,0) emission data and model fit. They attributed this greater than 5% deviation to an incident energy resolution issue near threshold, though it could also indicate a larger cascade contribution relative to the present results. Furthermore, renormalization of the LBH cross section of Ajello and Shemansky, using the recommended value for the H_2 Lyman α emission cross section at 100 eV of either *van der Burgt et al.* [1989] or *Liu et al.* [1998], would scale their cross section by factors of $\sim$0.892 or $\sim$0.875, respectively. Such (allowed) renormalization brings the cross section of *Ajello and Shemansky* [1985] into better agreement with the present results.

[33] More recently, *Budzien et al.* [1994] have inferred a 31% emission contribution (see their paper for a full discussion) to the total a $^1\Pi_g$ state excitation by means of "slow" cascade from the a′ $^1\Sigma_u^-$ and w $^1\Delta_u$ states based on observations of the airglow by the Ultraviolet Limb Imaging experiment of STS-39. The 31% "slow" cascade contribution to the total a $^1\Pi_g$ emission is in contrast with the (negligible) contribution suggested by *Ajello and Shemansky* [1985]. However, it should be stated that the field-of-view, chamber size, and pressure range employed in the a $^1\Pi_g$ emission investigation of *Ajello and Shemansky* [1985] should preclude contamination within stated errors of their LBH measurement by the "slow" cascade component. It is interesting to note that *Eastes and Dentamaro* [1996], and later *Eastes* [2000a, 2000b], have suggested that collisional induced electronic transitions (CIET) among the a $^1\Pi_g$, a′ $^1\Sigma_u^-$, and w $^1\Delta_u$ states of N_2 could be as important as radiative transitions among these states. Obviously, the revised ICSs in the present results impact the interpretation of the a $^1\Pi_g$, a′ $^1\Sigma_u^-$, and w $^1\Delta_u$ excitation-cascade-CIET systems and subsequent interpretation of atmospheric emissions.

[34] *Mason and Newell* [1987] have presented cross sections for the X $^1\Sigma_g^+$ - a $^1\Pi_g$ transition by detecting N_2 metastables (a $^1\Pi_g$) produced by electron impact with a channel electron multiplier in a TOF experiment. Their experiment produced a relative excitation function that was then normalized to an average of peak ICS values [*Borst*, 1972; *Cartwright et al.*, 1977b; *Ajello and Shemansky*, 1985] (which can be renormalized based on new data). In examining these data, it should be noted that the method does not account for processes such as cascade and predissociation that may take place during the flight time of the metastable molecules. It is also very possible that other metastable states were simultaneously detected since their detection technique lacked any suitable metastable state discrimination. Further, the error bars provided by *Mason and Newell* [1987] are significant underestimates of a true experimental error considering the detection method they used. For instance, variation in surface detection efficiency of their detector probably introduced an underestimated additional systematic error in their work, as did their metastable selectivity.

[35] Additional comments should be made with respect to the potential detection of metastables other than the a $^1\Pi_g$ state by *Mason and Newell* [1987]. They assumed that the only possible unwanted metastable contributors would be the A $^3\Sigma_u^+$ and E $^3\Sigma_g^+$ states. They argued that the A $^3\Sigma_u^+$ state would not be detected, based on threshold energy, due to the work function of their detection surface. Further, they stated the E $^3\Sigma_g^+$ state, although present and, in principle detectable, would not contribute as the cross section is approximately an order of magnitude lower than that of the a $^1\Pi_g$ state (apart from the resonance near 12–13 eV [*Borst et al.*, 1972]). However, the quoted work function of their detector, $\sim$8 eV, will allow detection of numerous metastables with sufficiently large excitation energies, cross sections, and long lifetimes such as the a′ $^1\Sigma_u^-$ and w $^1\Delta_u$ states, and possibly the upper vibrational levels (above $\sim$8 eV) of the A $^3\Sigma_u^+$ state (which can be excited both directly and by cascade from higher lying levels such as the B $^3\Pi_g$ state).

[36] *Mason and Newell* [1987] obtained a lifetime of $\sim$115 μs that was attributed to the a $^1\Pi_g$ state (see their paper for a full discussion) by accounting for in-flight decay of the metastables prior to detection. Though other lifetime measurements were available [e.g., *Lichten*, 1957; *Holland*, 1969; *Freund*, 1972; *Dahl and Oddershede*, 1986] from various techniques, their fitted lifetime was compared to the very similar lifetime of *Borst and Zipf* [1971] using the same TOF method for the purpose of metastable identification. A much smaller lifetime of $\sim$55 μs, as suggested by others [*Dahl and Oddershede*, 1986; *Marinelli et al.*, 1989; *Magne et al.*, 1992], would still enable a relatively significant sampling of the a $^1\Pi_g$ metastables given their experimental conditions. However, a lifetime on this order would suggest that additional metastable states, other than the a $^1\Pi_g$ state, would have been detected in their TOF experiment at long flight times. As discussed by *Marinelli et al.* [1989] (first by *Freund* [1972]), the a′ $^1\Sigma_u^-$ state is a strong candidate for contamination of the *Mason and Newell* [1987] a $^1\Pi_g$ TOF spectra. Accounting for other metastable states would explain the early peak onset and the fast rise from threshold in the data of *Mason and Newell* [1987]. Furthermore, it is unfortunate that a near-threshold excitation function was not presented by *Mason and Newell* [1987]. This could have allowed a clearer assessment of what metastable states may have contaminated their measurements (assuming an adequately small incident energy spread and reasonably comparable metastable yields for contributing states). Of note, Mason and Newell later modified their instrument to specifically enable metastable state selection [*Mason and Newell*, 1991].

4.7. X $^1\Sigma_g^+$ - w $^1\Delta_u$

[37] ICSs for excitation of the w $^1\Delta_u$ state measured by *Cartwright et al.* [1977b; *Trajmar et al.*, 1983] and *Campbell et al.* [2001] agree well with the present results (Figure 8) at 20 eV. However, the excitation function suggested by these other two measurements indicate a larger peak ICS and a faster fall-off with increasing energy than ours. The theoretical ICSs of *Chung and Lin* [1972] show disagreement with all of the three experimental data sets discussed above.

4.8. X $^1\Sigma_g^+$ - C $^3\Pi_u$

[38] Figure 9 shows ICSs for excitation of the C $^3\Pi_u$ state. All experimental data sets are generally in agreement at higher energies. Again, the present data indicate a cross section with a lower peak than other measurements. This is significant since this transition gives rise to the UV emissions of the second positive band system (C $^3\Pi_u$ - B $^3\Pi_g$) with further cascade to the metastable A $^3\Sigma_u^+$ state. The above observation could indicate a larger cascade, by available mechanisms, into the C $^3\Pi_u$ state from higher lying Rydbergs compared to previous data sets.

[39] *Poparic et al.* [1999] (from the tabulation by *Brunger and Buckman* [2002]) have derived ICSs from differential (in angle) impact energy excitation function scans (threshold to 17 eV) of the $v' = 0$, 1, and 2 levels of the C $^3\Pi_u$ state measured at forward scattering by making assumptions regarding the angular distributions of scattered electrons. These data [*Poparic et al.*, 1999] show a steeper rise in the cross section than what is observed in the present data. However, their ad hoc assumption of isotropic electron scattering systematically favors their analysis toward the results of *Campbell et al.* [2001]. This assumption reflects the relatively flat DCSs obtained by *Brunger and Teubner* [1990] over a limited angular range, which were used to obtain the ICSs of *Campbell et al.* [2001]. The DCSs of *Khakoo et al.* [2005] and others [e.g., *Cartwright et al.*, 1977a; *Trajmar et al.*, 1983; *Zubek and King*, 1994] do not support the assumption of isotropic electron scattering.

[40] After a peak around 14 eV, these cross sections [*Poparic et al.*, 1999] agree within uncertainties with the data of both *Cartwright et al.* [1977b; *Trajmar et al.*, 1983] and *Campbell et al.* [2001]. Extrapolation of the excitation to higher energies also apparently supports the results of *Zubek and King* [1994]. *Zubek* [1994] estimated ICSs based on a broadband (240–400 nm) optical emission excitation function. Zubek claims that the published cross sections are equivalent to ICSs such as those determined here. However, this will only be true in the case where there is no cascade contribution to the C $^3\Pi_u$ state excitation (from higher- and near-lying Rydberg states) and there is no significant branching to channels outside that of the measured optical emissions. In making this claim, Zubek refers to *Shaw and Campos* [1983], who concluded that there was little or no radiative cascade based on their delayed coincidence experiments with pulsed electron excitation. The Shaw and Campos experiment was conducted at relatively high target pressures (10^{-2}–10^{-3} Torr) where systematic effects such as collisional cascade, collisional induced electronic transitions, and radiation trapping are known to occur [*Tohyama and Nagata*, 2005]. Unfortunately, no evidence is presented by *Shaw and Campos* [1983] to confirm that these effects were not present in their measurement. Therefore it is difficult to assess the validity of the "single-collision condition" in their experiment.

[41] Zubek quotes a prohibitively small error, or "standard deviation," in his measurement, i.e., 3.5%. This is unrealistically low for a cross section derived by electron impact induced optical emission spectroscopy. If a more realistic error bar had been assigned, more definitive comparisons could be made. Of note, if the Zubek data were scaled downward (i.e., reduced by 14.9% following the arguments presented by *Itikawa* [2005]), their consistency with the present data would be significantly improved. Additionally, the early calculation of *Chung and Lin* [1972] shows agreement with our ICSs at intermediate energies but diverges near threshold and at larger impact energies.

4.9. Sum

[42] Figure 10 gives the total summed cross section for all states studied in the present work. The summed cross sections presented here were determined by integrating the summed DCSs reported by *Khakoo et al.* [2005] and not by summing the individual ICSs determined in the present work (although both methods give nearly identical results). Thus the presented sum ICSs are independent of any systematic errors introduced by the unfolding procedure employed by *Khakoo et al.* [2005]. *Cartwright et al.* [1977b; *Trajmar et al.*, 1983] and *Campbell et al.* [2001] are the only other works in the literature that present ICSs for all the states studied here. Therefore summed cross sections based on these experiments are included in the figure. Remarkable agreement is seen between all three data sets for energies $\geq$20 eV. Since there are discrepancies among the individual cross sections for the individual states at these energies, this observation indicates that these experiments likely produced very similar energy loss spectra while the measured spectra were not unfolded consistently amongst each other. The present data fall below the other data sets by a factor of $\sim$2 at the cross section peak and agree with the *Cartwright et al.* [1977b; *Trajmar et al.*, 1983] datum at 10 eV. This indicates that at lower energies there could be discrepancies between the raw energy loss spectra, which is perhaps not surprising at these incident energies. Additionally, the discrepancies could be indicative of whether or not flux-weighted FC factors were used in the employed unfolding method.

5. Conclusions

[43] ICSs for electron impact excitation of the X $^1\Sigma_g^+$ to A $^3\Sigma_u^+$, B $^3\Pi_g$, W $^3\Delta_u$, B′ $^3\Sigma_u^-$, a′ $^1\Sigma_u^-$, a $^1\Pi_g$, w $^1\Delta_u$, and C $^3\Pi_u$ transitions at impact energies between 10 and 100 eV were derived from DCS results [*Khakoo et al.*, 2005]. New DCSs for excitation of the a $^1\Pi_g$ state have been measured at 200 eV and a corresponding ICS has been derived. Generally, the ICS data are in reasonable accord with previous experimental efforts at 30 eV and above. However, at lower energies, from threshold through the excitation function peak regions, the present ICSs tend to be smaller than previous results. Given that secondary electron fluxes in the atmospheres of Earth and Titan peak at these lower energies, the present results have potentially significant

implications on our understanding of UV emissions in these environments. This general trend in the agreement among the evaluated data sets is not evident in the DCSs from which the present ICSs and those of other works discussed were derived [*Cartwright et al.*, 1977a; *Zetner and Trajmar*, 1987; *Brunger and Teubner*, 1990; *Khakoo et al.*, 2005]. This observation emphasizes the well recognized fact that DCSs provide significantly more detail regarding the physics of the collisional excitation process.

[44] One of the main motivations for the present ICS determinations was the observed discrepancies among the underlying DCSs. After extensively reviewing the literature throughout the course of this work, it has become apparent that there is a need for new theoretical work in this area. It is hoped that the new DCSs of *Khakoo et al.* [2005] and the present ICSs will spur scattering theorists to revisit the problem of electron impact excitation of N_2 at the DCS level. Furthermore, the present results, particularly the lower ICSs for excitation of the a $^1\Pi_g$ and C $^3\Pi_u$ states, have potentially significant implications on our understanding of UV emissions that result from excitation of the states studied here in the atmospheres of Earth and Titan.

[45] **Acknowledgments.** The work was performed at the California State University, Fullerton (CSUF) and at the Jet Propulsion Laboratory (JPL), California Institute of Technology, under a contract with the National Aeronautics and Space Administration (NASA). Financial support through NASA's Planetary Atmospheres program and the National Science Foundation (grants NSF ATM-0131210 and NSF-PHY-RUI-0096808) is gratefully acknowledged. This research was performed while CPM held a National Research Council Research Associateship Award at JPL.

[46] Arthur Richmond thanks Laurence Campbell and Richard Eastes for their assistance in evaluating this paper.

References

Ajello, J. M. (1970), Emission cross sections of N_2 in vacuum ultraviolet by electron impact, *J. Chem. Phys.*, *53*(3), 1156–1165.

Ajello, J. M., and D. E. Shemansky (1985), A reexamination of important N_2 cross-sections by electron-impact with application to the dayglow: The Lyman-Birge-Hopfield band system and N I (119.99 nm), *J. Geophys. Res.*, *90*(A10), 9845–9861.

Benesch, W., J. T. Vanderslice, S. G. Tilford, and P. G. Wilkinson (1965), Potential curves for observed states of N_2 below 11 eV, *Astrophys. J.*, *142*(3), 1227–1240.

Borst, W. L. (1972), Excitation of several important metastable states of N_2 by electron-impact, *Phys. Rev. A*, *5*(2), 648–656.

Borst, W. L., and E. C. Zipf (1971), Lifetimes of metastable CO and N_2 molecules, *Phys. Rev. A*, *3*(3), 979–989.

Borst, W. L., W. C. Wells, and E. C. Zipf (1972), Excitation of metastable E $^3\Sigma_g^+$ state of N_2 by electron-impact, *Phys. Rev. A*, *5*(4), 1744–1747.

Brinkman, R. T., and S. Trajmar (1970), Electron impact excitation of N_2, *26*(1), 201–207.

Brunger, M. J., and S. J. Buckman (2002), Electron-molecule scattering cross-sections. I. Experimental techniques and data for diatomic molecules, *Phys. Rep.*, *357*(3-5), 215–458.

Brunger, M. J., and P. J. O. Teubner (1990), Differential cross-sections for electron-impact excitation of the electronic states of N_2, *Phys. Rev. A*, *41*(3), 1413–1426.

Brunger, M. J., S. J. Buckman, and M. T. Elford (2003), Integral elastic cross sections, in *Landolt-Bornstein Group 1: Elementary Particles, Nuclei, and Atoms*, vol. 17, subvol. C, edited by Y. Itikawa, pp. 6052–6084, Springer, New York.

Budzien, S. A., P. D. Feldman, and R. R. Conway (1994), Observations of the far-ultraviolet airglow by the ultraviolet limb imaging experiment on STS-39, *J. Geophys. Res.*, *99*(A12), 23,275–23,287.

Campbell, L., M. J. Brunger, A. M. Nolan, L. J. Kelly, A. B. Wedding, J. Harrison, P. J. O. Teubner, D. C. Cartwright, and B. McLaughlin (2001), Integral cross sections for electron impact excitation of electronic states of N_2, *J. Phys. B At. Mol. Opt. Phys.*, *34*(7), 1185–1199.

Cartwright, D. C., A. Chutjian, S. Trajmar, and W. Williams (1977a), Electron-impact excitation of electronic states of N_2: 1. Differential cross-sections at incident energies from 10 to 50 eV, *Phys. Rev. A*, *16*(3), 1013–1040.

Cartwright, D. C., S. Trajmar, A. Chutjian, and W. Williams (1977b), Electron-impact excitation of electronic states of N_2: 2. Integral cross-sections at incident energies from 10 to 50 eV, *Phys. Rev. A*, *16*(3), 1041–1051.

Childers, J. G., K. E. James, I. Bray, M. Baertschy, and M. A. Khakoo (2004), Low-energy electron scattering from atomic hydrogen. I. Ionization, *Phys. Rev. A*, *69*(2), 022709.

Chung, S., and C. C. Lin (1972), Excitation of electronic states of nitrogen molecule by electron-impact, *Phys. Rev. A*, *6*(3), 988–1002.

Dahl, F., and J. Oddershede (1986), Radiative lifetime of the forbidden a $^1\Pi_g$ -X $^1\Sigma_g^+$ transition of N_2, *Phys. Scr.*, *33*(2), 135–140.

Eastes, R. W. (2000a), Emissions from the N_2 Lyman-Birge-Hopfield bands in the Earth's atmosphere, *Phys. Chem. Earth, Part C*, *25*(5–6), 523–527.

Eastes, R. W. (2000b), Modeling the N_2 Lyman-Birge-Hopfield bands in the dayglow: Including radiative and collisional cascading between the singlet states, *J. Geophys. Res.*, *105*(A8), 18,557–18,573.

Eastes, R. W., and A. V. Dentamaro (1996), Collision-induced transitions between the a $^1\Pi_g$, a′ $^1\Sigma_u^-$, and w $^1\Delta_u$ states of N_2: Can they affect auroral N_2 Lyman-Birge-Hopfield band emissions?, *J. Geophys. Res.*, *101*(A12), 26,931–26,940.

Finn, T. G., and J. P. Doering (1976), Measurement of 13 to 100 eV electron-impact excitation cross-section for X $^1\Sigma_g^+$ - a $^1\Pi_g$ transition in N_2, *J. Chem. Phys.*, *64*(11), 4490–4494.

Fliflet, A. W., V. McKoy, and T. N. Rescigno (1979), Cross-sections for excitation of the $B^3\Pi_g$, $C^3\Pi_u$ and $E^3\Sigma_g^+$ states of N_2 by low-energy electron-impact in the distorted-wave approximation, *J. Phys. B At. Mol. Opt. Phys.*, *12*(19), 3281–3293.

Freund, R. S. (1972), Radiative lifetime of N_2 (a $^1\Pi_g$) and formation of metastable N_2 (a′ $^1\Sigma_u$), *J. Chem. Phys.*, *56*(9), 4344–4351.

Gillan, C. J., J. Tennyson, B. M. McLaughlin, and P. G. Burke (1996), Low-energy electron impact excitation of the nitrogen molecule: Optically forbidden transitions, *J. Phys. B At. Mol. Opt. Phys.*, *29*(8), 1531–1547.

Gote, M., and H. Ehrhardt (1995), Rotational-excitation of diatomic-molecules at intermediate energies: Absolute differential state-to-state transition cross-sections for electron-scattering from N_2, Cl_2, CO and HCl, *J. Phys. B At. Mol. Opt. Phys.*, *28*(17), 3957–3986.

Holland, R. F. (1969), Excitation of nitrogen by electrons: Lyman-Birge-Hopfield system of N_2, *J. Chem. Phys.*, *51*(9), 3940–3950.

Holley, T. K., S. Chung, C. C. Lin, and E. T. P. Lee (1981), Electron-impact excitation cross-sections of the a $^1\Pi_g$ of the N_2 molecule by the close-coupling method, *Phys. Rev. A*, *24*(6), 2946–2952.

Hughes, M., K. E. James, J. G. Childers, and M. A. Khakoo (2003), Accurate determination of background scattered electrons in crossed electron- and gas-beam experiments using a movable gas beam source, *Meas. Sci. Technol.*, *14*(6), 841–845.

Huo, W. M., and C. E. Dateo (1999), Finite Z-matrix calculation of electron-N_2 collisions, paper presented at XXI International Conference on Photonic, Electronic and Atomic Collisions, Int. Union of Pure and Appl. Phys., Sendai, Japan.

Itikawa, Y. (2005), Cross sections for electron collisions with nitrogen molecules, *J. Phys. Chem. Ref. Data*, in press.

Itikawa, Y., M. Hayashi, A. Ichimura, K. Onda, K. Sakimoto, K. Takayanagi, M. Nakamura, H. Nishimura, and T. Takayanagi (1986), Cross-sections for collisions of electrons and photons with nitrogen molecules, *J. Phys. Chem. Ref. Data*, *15*(3), 985–1010.

Johnson, P. V., I. Kanik, M. A. Khakoo, J. W. McConkey, and S. S. Tayal (2003), Low energy differential and integral electron-impact cross sections for the $2s^22p^4\ P_3 \rightarrow 2p^33s\ S_3^o$ excitation in atomic oxygen, *J. Phys. B At. Mol. Opt. Phys.*, *36*(21), 4289–4299.

Khakoo, M. A., C. E. Beckmann, S. Trajmar, and G. Csanak (1994), Electron-impact excitation of the $ns[3/2]^o_{J=2,1}$ and $ns'[1/2]^o_{J=0,1}$ levels of Ne, Ar, Kr and Xe, *J. Phys. B At. Mol. Opt. Phys.*, *27*(14), 3159–3174.

Khakoo, M. A., P. V. Johnson, I. Ozkay, P. Yan, S. Trajmar, and I. Kanik (2005), Differential cross sections for the electron impact excitation of the $A^3\Sigma_u^+$, $B^3\Pi_g$, $W^3\Delta_u$, $B'\ ^3\Sigma_u^-$, a′ $^1\Sigma_u^-$, $a^1\Pi_g$, $w^1\Delta_u$ and $C^3\Pi_u$ states of N_2, *Phys. Rev. A*, *71*, 062703.

LeClair, L. R., and S. Trajmar (1996), Absolute inelastic differential electron scattering cross sections for He, Xe, N_2 and CO at near-threshold impact energies for 90 degrees scattering angle, *J. Phys. B At. Mol. Opt. Phys.*, *29*(22), 5543–5566.

Lichten, W. (1957), Lifetime measurements of metastable states in molecular nitrogen, *J. Chem. Phys.*, *26*(2), 306–313.

Liu, X. M., D. E. Shemansky, S. M. Ahmed, G. K. James, and J. M. Ajello (1998), Electron-impact excitation and emission cross sections of the H_2 Lyman and Werner systems, *J. Geophys. Res.*, *103*(A11), 26,739–26,758.

Lofthus, A., and P. H. Krupenie (1977), The spectrum of molecular nitrogen, *J. Phys. Chem. Ref. Data*, *6*(1), 113–307.

Magne, L., G. Cernogora, and P. Veis (1992), Relaxation of metastable N_2 ($a\ ^1\Pi_g$, $v' = 0–2$) in nitrogen afterglow, *J. Phys. D Appl. Phys.*, *25*(3), 472–476.

Marinelli, W. J., W. J. Kessler, B. D. Green, and W. A. M. Blumberg (1989), The radiative lifetime of $N_2(a\ ^1\Pi_g, v = 0–2)$, *J. Chem. Phys.*, *91*(2), 701–707.

Mason, N. J., and W. R. Newell (1987), Electron-impact total excitation cross-section of the $a\ ^1\Pi_g$ state of N_2, *J. Phys. B At. Mol. Opt. Phys.*, *20*(15), 3913–3921.

Mason, N. J., and W. R. Newell (1991), A state selective metastable detector, *Meas. Sci. Technol.*, *2*(6), 568–570.

Nickel, J. C., C. Mott, I. Kanik, and D. C. McCollum (1988), Absolute elastic differential electron-scattering cross-sections for carbon-monoxide and molecular nitrogen in the intermediate energy region, *J. Phys. B At. Mol. Opt. Phys.*, *21*(10), 1867–1877.

Poparic, G., M. Vicic, and D. S. Belic (1999), Vibrational excitation of the $C\ ^3\Pi_u$ state of N_2 by electron impact, *Chem. Phys.*, *240*(1-2), 283–289.

Shaw, M., and J. Campos (1983), Emission cross-sections of the 2nd positive and 1st negative systems of N_2 and N_2^+ excited by electron-impact, *J. Quant. Spectrosc. Radiat. Transf.*, *30*(1), 73–76.

Shemansky, D. E., J. M. Ajello, and D. T. Hall (1985), Electron-impact excitation of H_2-Rydberg band systems and the benchmark dissociative cross-section for H-Lyman-alpha, *Astrophys. J.*, *296*(2), 765–773.

Shyn, T. W., and G. R. Carignan (1980), Angular-distribution of electrons elastically scattered from gases: 1.5–400 eV on N_2, *Phys. Rev. A*, *22*(3), 923–929.

Tanaka, Y., M. Ogawa, and A. S. Jursa (1964), Forbidden absorption-band systems of N_2 in vacuum-ultraviolet region, *J. Chem. Phys.*, *40*(12), 3690–3700.

Tohyama, Y., and T. Nagata (2005), Electron impact emission of $N_2\ ^2P(v', v'')$ bands studied under single-collision condition, *J. Phys. Soc. Jpn.*, *74*(1), 326–332.

Trajmar, S., and D. C. Cartwright (1984), Excitation of molecules by electron impact, in *Electron-Molecule Interactions and Their Applications*, edited by L. G. Christophourou, pp. 155–249, Elsevier, New York.

Trajmar, S., D. F. Register, and A. Chutjian (1983), Electron-scattering by molecules: 2. Experimental methods and data, *Phys. Rep.*, *97*(5), 221–356.

van der Burgt, P. J. M., W. B. Westerveld, and J. S. Risley (1989), Photoemission cross-sections for atomic transitions in the extreme ultraviolet due to electron collisions with atoms and molecules, *J. Phys. Chem. Ref. Data*, *18*(4), 1757–1805.

Wrkich, J., D. Matthews, I. Kanik, S. Trajmar, and M. A. Khakoo (2002), Differential cross-sections for the electron impact excitation of the $B\ ^1\Sigma_u^+$, $c\ ^3\Pi_u$, $a\ ^3\Sigma_g^+$, $C\ ^1\Pi_u$, E, $F\ ^1\Sigma_g^+$ and $e\ ^3\Sigma_u^+$ states of molecular hydrogen, *J. Phys. B At. Mol. Opt. Phys.*, *35*(22), 4695–4709.

Zecca, A., G. P. Karwasz, and R. S. Brusa (1996), One century of experiments on electron-atom and molecule scattering: A critical review of integral cross-sections: 1. Atoms and diatomic molecules, *Riv. Nuovo Cimento Soc. Ital. Fis.*, *19*(3), 1–146.

Zetner, P. W., and S. Trajmar (1987), Electron impact excitation cross sections for molecular electronic states at low energies, paper presented at XV International Conference on Photonic, Electronic, and Atomic Collisions, Int. Union of Pure and Appl. Phys., Brighton, UK.

Zubek, M. (1994), Excitation of the $C^3\Pi_u$ state of N_2 by electron-impact in the near-threshold region, *J. Phys. B At. Mol. Opt. Phys.*, *27*(3), 573–581.

Zubek, M., and G. C. King (1994), Differential cross-sections for electron-impact excitation of the $C^3\Pi_u$, $E^3\Sigma_g^+$ and $a''^1\Sigma_g^+$ states of N_2, *J. Phys. B At. Mol. Opt. Phys.*, *27*(12), 2613–2624.

P. V. Johnson, I. Kanik, and C. P. Malone, Jet Propulsion Laboratory, California Institute of Technology, Pasadena, CA 91109, USA. (paul.v.johnson@jpl.nasa.gov)

M. A. Khakoo and K. Tran, Department of Physics, California State University, Fullerton, CA 92834, USA.